Use of Mechanical Modeling To Study Multiphase Polymeric Materials

D. Colombini,† G. Merle,* and N. D. Alberola

Laboratoire Matériaux Organiques à Propriétés Spécifiques, UMR−CNRS 5041/Université de Savoie, 73376 Le Bourget du Lac, Cedex, France

Received January 16, 2001

ABSTRACT: Viscoelastic properties of several multiphase polymeric materials were investigated in connection with their morphologies. Both mechanical modeling and mechanical spectrometry were used as tools for extracting information about morphology, molecular mobility, and interfacial interactions in such heterogeneous systems. The use of self-consistent mechanical models in direct and reverse modes was shown to be of interest for in depth discussion of the possibilities and limitations of the theoretical mechanical approach in the understanding of experimental dynamic mechanical data of complex polymeric materials. Christensen and Lo's model was used in direct mode to highlight mechanical coupling effects in binary thermoset/thermoplastic polymer blends. It was shown that the magnitude of these effects between phases in such blends, as in composite materials, depends not only on mechanical properties and relative content of each phase but also on the geometric arrangement of the polymeric phases. Furthermore, a new way of presenting experimental dynamic mechanical data and simulations resulting from direct mechanical approach, was also proposed as a qualitative, well-suited probe of morphology of multicomponent polymeric materials. The models of Christensen and Lo and of Herve and Zaoui were both used in reverse mode. It was demonstrated that such a new approach for mechanical modeling allows the extraction of the actual viscoelastic properties of one phase among others in multiphase polymeric materials. That is of particular interest for investigating the actual properties of the interfacial area in such complex systems, whose experimental in situ detection and characterization remain problem.

1. Introduction

In general, two or more polymers may be blended to form a wide variety of random or structured morphologies in order to obtain materials which can combine the characteristics of both components. This is an important technical advantage since polymer blends allow production of new materials by using preexisting others, thus reducing development costs. However, it may be difficult or impossible in practice to achieve these potential combinations through simple blending: as a matter of fact, most polymers are thermodynamically immiscible and form heterogeneous multiphase systems with weak physical and chemical interactions between the phases and poor overall properties. An improvement is achieved by introducing a so-called compatibilizer, such as a block or graft copolymer, which interacts with the other polymers and so offers new properties to the blends.[1−3] The compatibilizer is considered to be located mainly at the interface between the two immiscible polymers, where in many cases it induces local miscibility. It may provide an increased adhesion and an enlarged volume of the interdiffusion layer, and also reduce the interfacial energy between the phases. This process often results in a stable and finer dispersion of the minor component into the other and leads to the formation of an interphase zone between the continuous and the dispersed phases. This area can be defined as a topological region showing a given thickness in the vicinity of the dispersed phase. Obviously, the properties of such an interfacial region differ from those of the pure components and strongly affect the overall properties of the resulting multiphase material. As a consequence, an interphase may be considered to have a certain volume with its own characteristic properties or property gradients. Although the concept of the interphase is rapidly gaining acceptance, its in situ detection and characterization remain a problem. Dynamic mechanical spectrometry was shown to be an excellent way[4−7] for such a purpose, insofar as this technique allows a complete exploration of relaxational mechanisms in viscoelastic materials.

The present work concerns the use and optimalization of mechanical models and dynamic mechanical analysis, as tools for extracting information about morphology, molecular mobility, and interfacial interactions in multicomponent polymeric systems. The objective of the work is to deduce this information from the response of these complex materials to dynamic mechanical fields and the knowledge of their composition and properties of their components. Despite the widespread use of dynamic mechanical analytical instruments, the interpretation of the results for more complex polymeric materials, such as binary polymer blends or three-phase compatibilized polymer blends, is much more difficult. Correct interpretations are only possible when a specialized knowledge of the technique itself together with a thorough understanding of the effective theoretical response of these materials to dynamic fields, is accounted for. As a matter of fact, even if it is well understood that mechanical and viscoelastic properties of heterogeneous polymeric systems depend on molecular relaxation processes, it is also important to recall that mechanical spectra reflect the overall viscoelastic behavior of multiphase materials. Each viscoelastic response is therefore governed by two major factors: (1) the nature of bonds between components[5−8] and (2) mechanical coupling effects between phases.[8−15] Thus, before interpreting changes on the viscoelastic behavior of blended component, it is first necessary to predict the

* Corresponding author.
† Present address: Department of Polymer Science and Engineering, Centre for Chemistry and Chemical Engineering, Lund Institute of Technology, Lund University, Box 124/Getingevägen 60, 22100 Lund, Sweden.

10.1021/ma010076v CCC: $20.00
Published on Web 07/12/2001

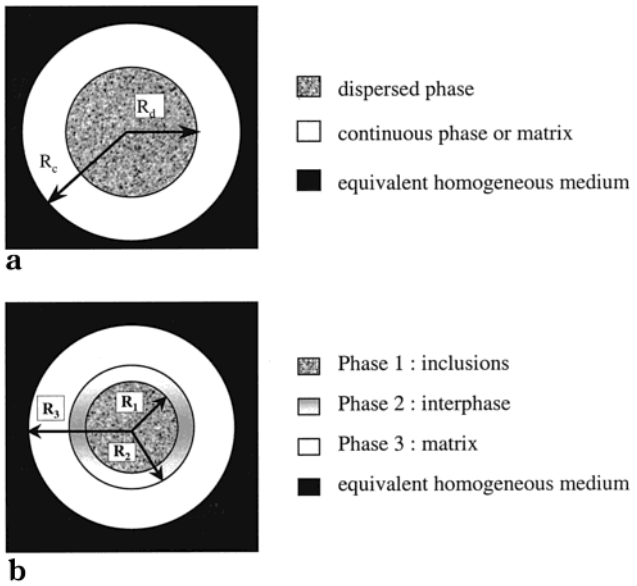

Figure 1. Illustrations of the Representative Volume Elements (RVE) considered in this work: (a) RVE-2 phases for binary systems; (b) RVE-3 phases for ternary systems.

sole effects resulting from mechanical coupling between phases.

The mechanical models used in this paper are based on the $(n + 1)$ phase self-consistent scheme.[16,17] The present investigation requires the use of self-consistent mechanical models in *direct* and *reverse* modes. In this way, the two modes are first detailed and then applied to several polymer blends and composite materials, to give evidence that mechanical modeling can improve the ability of experimental viscoelastic data of multiphase polymeric materials to reveal information about the overall properties of such heterogeneous materials.

2. Mechanical Modeling

2.1. Presentation of Mechanical Models. The prediction of the complex moduli of multiphase materials (polymer blends and composites) is usually based on phenomenological laws,[18] variational methods,[19−21] or self-consistent schemes[16,17] extended to describe the viscoelastic behavior[8,13−14,22−26] through the correspondence principle.[27]

The mechanical models used in this work are based on the $(n + 1)$ phase self-consistent scheme and are here applied for a two-layer[16] concentric sphere and a three-layer[17] phase concentric sphere. Such approaches, which were first presented by Christensen and Lo[16] and Herve and Zaoui,[17] are based on the following assumptions:

- The inclusions are randomly dispersed in the matrix.
- Each phase is homogeneous and isotropic, whatever the observation scale.
- Bondings between neighboring phases are perfect.

Self-consistent schemes require the definition of representative volume element (RVE). The RVE-2 phases and RVE-3 phases are depicted in Figure 1, parts a and b, and consist of two- or three concentric spheres embedded in a equivalent homogeneous medium, respectively. In RVE-2 phases (Figure 1a), the dispersed phase, acting as the central core with the radius R_d, is embedded by a shell of the continuous phase or matrix that is limited by the spheres with the radii R_d and R_c. The ratios of radii are expressed as a function of the volume fractions of the dispersed (V_d) and continuous (V_c) phases as follows:

$$V_d = R_d^3/R_c^3 \quad \text{and} \quad V_c = 1 - (R_d^3/R_c^3) \tag{1}$$

In RVE-3 phases (Figure 1b), the central core (phase 1) consists of inclusions with the radius R_1. Phase 1 is surrounded by a shell of interphase (phase 2), which is limited by the spheres with the radii R_1 and R_2. Phase 2 is covered by a shell of matrix (phase 3), which is limited by the spheres with the radii R_2 and R_3. The ratios of radii are also expressed as a function of the volume fractions of the different phases, denoted as V_1, V_2, and V_3, respectively.

$$V_1 = R_1^3/R_3^3, \quad V_2 = (R_2^3 - R_1^3)/R_3^3, \quad \text{and} \quad V_3 = 1 - (R_2^3/R_3^3) \tag{2}$$

Then, as usual for self-consistent schemes, prediction of the elastic and the linear viscoelastic properties of such multicomponent polymeric materials is based on the derivation of the elastic strain or stress field in an infinite medium consisting of a two- or three-layer inclusion embedded in a matrix submitted to uniform stress or strain at the infinity.

Bulk Modulus. The external stress field applied to calculate the bulk modulus, K, of the homogeneous material is a hydrostatic pressure on its outer boundary. The general equations of displacements and stresses are solved by means of the continuity conditions on displacements or stresses at interfaces. Finally, according to the correspondence principle,[27] the complex bulk modulus, K^*, of the two-[16] or the three-layered[17] concentric sphere (denoted as $K^*_{2\ \text{phases}}$ or $K^*_{3\ \text{phases}}$, respectively) is given by

$$K^*_{2\ \text{phases}} = K^*_c + \frac{V_d(K^*_d - K^*_c)}{1 + (1 - V_d)\left[\frac{(K^*_d - K^*_c)}{\left(K^*_c + \frac{4}{3}G^*_c\right)}\right]} \tag{3}$$

and

$$K^*_{3\ \text{phases}} = K^*_3 + [(3K^*_3 + 4G^*_3)R_2^3((K^*_1 - K^*_2)R_1^3(3K^*_3 + 4G^*_2) + (K^*_2 - K^*_3)R_2^3(3K^*_1 + 4G^*_2))]/[3(K^*_2 - K^*_1)R_1^3(R_2^3(3K^*_3 + 4G^*_2) + 4R_3^3(G^*_3 - G^*_2)) + (3K^*_1 + 4G^*_2)R_2^3(3R_2^3(K^*_3 - K^*_2) + R_3^3(3K^*_2 + 4G^*_3))] \tag{4}$$

where the subscripts c, d, 1, 2, and 3 are in accordance with those used in the corresponding RVE depicted in Figure 1a,b.

Shear Modulus. In a similar way, the solution for the complex shear modulus, G^*, of the two- or the three-layered concentric sphere (denoted as $G^*_{2\ \text{phases}}$ or $G^*_{3\ \text{phases}}$, respectively) is given by the resolution of the following quadratic equation:

$$A\left[\frac{G^*}{G^*_{\text{matrix}}}\right]^2 + B\left[\frac{G^*}{G^*_{\text{matrix}}}\right] + C = 0 \tag{5}$$

The determination of the constants A, B, and C are given in the Appendix for both two- and three-phases mechanical models. G^*_{matrix} corresponds to the complex shear modulus of the component which is considered as

the last surrounding phase in the model, i.e., G^*_c (Figure 1a) or G^*_3 (Figure 1b), respectively.

2.2. *Direct* and *Reverse* Mechanical Modeling. The use of self-consistent mechanical models in direct and reverse modes is great of interest for giving an in depth description and discussion of the possibilities and limitations of the theoretical mechanical approach in the understanding of dynamic mechanical data of complex multiphase polymeric materials. First, both direct and reverse mechanical modeling have to be detailed.

Direct mechanical modeling is the usual mode of use.[11,12,14,22−24] Such a way leads to the prediction of the viscoelastic properties of a multiphase material from the knowledge of the viscoelastic properties of all pure components. Obviously, composition as well as morphology of the material are also required for numerical simulations. Thus, direct mechanical modeling permits to highlight the mechanical coupling effects between phases in connection with morphology. It was shown[12,14] that the magnitude of these effects between phases depends not only on mechanical properties and relative content of each phase but also on the geometric arrangement of the phases.

The reverse mode was recently proposed[13,25] and permits the extraction of the actual viscoelastic characteristics of one phase among others in an heterogeneous polymeric system,[13,25,26,28] by using the experimental viscoelastic properties of the multiphase material. Such a new approach for mechanical modeling was previously well tested[25,29] on model systems for which the viscoelastic characteristics, as well as the volume fractions, of all the components were exactly known. Thus, such a reverse way is an appropriate tool for estimating the actual viscoelastic properties of interphases, and could be of particular interest for investigating in situ synthesized interphases in reactive polymer blends or composites. Furthermore, as the composition of the experimental multiphase materials are usually known, the reverse approach could also be used to estimate the effective composition of these systems.

3. Materials and Sample Characterization

3.1. Materials. The choice of various multiphase polymeric materials is relevant to demonstrate the ability and the consistency of both direct and reverse approaches, whatever the study of heterogeneous polymeric systems may be. In this way, the present paper deals with several complex materials, such as binary and ternary polymer blends and particulate composites. Some details concerning these materials are here given.

Binary Thermoset and Thermoplastic Polymer Blends. The thermoset and thermoplastic blends used are made up of the diglycidyl ether of Bisphenol A (DGEBA; Dow Chemical [Midland, MI]; DER 332, $M_n = 348.5$ g/mol) and 4,4′-methylene bis[3-chloro-2,6-diethylaniline] (MCDEA; Lonza [Basel, Switzerland], $M_n = 380$ g/mol). Components were mixed at the stoichiometric ratio amino to hydrogen to epoxy equal to 1.

The high-T_g thermoplastic used was an amorphous nonfunctionalized polyetherimide supplied by General Electric Company [Pittsfield, MA] (PEI Ultem 1000, $M_n = 26$ kg/mol, $M_w = 50$ kg/mol). The mixture with PEI being miscible at 80 °C, the phase separation occurred during curing.

Preparation and kinetic study of such modified epoxy systems were reported elsewhere.[30] Precure time (120 h at 80 °C) was chosen to be longer than vitrification times to be sure that most of the microstructure developed isothermally. To ensure a complete network formation without any degradation, these samples were last postcured at 185 °C for 2 h.

In this paper, two binary polymer blends are investigated and denoted as BB10 and BB20, respectively. For example, BB10 denotes the system DGEBA−MCDEA modified with 10 wt % of PEI. Their morphologies, which were generated through the reaction-induced phase-separation procedure, were also investigated[31] by transmission electron microscopy (TEM). It was shown for the BB10 sample that phase separation induced a particulate morphology, with a thermoplastic-rich phase dispersed in a thermoset-rich continuous phase. On the opposite, with 20 wt % of PEI, phase separation led to the formation of an inverted structure with a continuous phase that is mainly rich in thermoplastic.

Particulate Composite. The particulate composite is constituted by a polymeric matrix (polystyrene; Elf-Atochem [Serquigny, France]; $M_n = 90$ kg/mol, $M_w = 260$ kg/mol) reinforced by 15 vol % of rigid inorganic inclusions (glass beads, Microperl 050−20, Sovitec [Florange, France]). Throughout this paper, this particulate composite is denoted as PC15.

The sample preparation was given previously,[8] and it was demonstrated[12] that such a volume fraction of spherical particles is lower than the percolation threshold (0.2). As a consequence, this PS/glass beads composite can be considered as a two-phase material in which polystyrene acts as the continuous phase.

Three-Phase in Situ Compatibilized Thermoset/Thermoplastic Polymer Blend. The epoxy prepolymer DGEBA and the diamine hardener MCDEA were also used for preparing a compatibilized epoxy/thermoplastic polymer blend.

The high-T_g thermoplastic used was poly(phenylene ether) (PPE 800: General Electric, MA; $M_n = 12$ kg/mol, $M_w/M_n = 2$).

The compatibilizer, denoted as MCDEA-*g*-K, used was based on a grafted maleic anhydride (MA) triblock copolymer poly(styrene-*b*-ethylene-*co*-butene-*b*-styrene) [P(S-*b*-EB-*b*-S)]. P(S-*b*-EB-*b*-S) was a commercial triblock copolymer from Shell Chemical Company (Houston, TX) (designated Kraton FG, $M_n = 52.5$ kg/mol [PS 7.5 kg/mol; PEB 37.5 kg/mol], $f_n(MA) = 10.4$, wt % (MA) = 1.94). MA functions were reacted with the diamine MCDEA to link the block copolymer to the epoxy network by means of the central block, whereas the PS blocks are miscible with PPE.

The compatibilized epoxy/thermoplastic polymer blend contained 1.5 wt % of MCDEA-*g*-K in a DGEBA−MCDEA network that contains 10 wt % of PPE. In the next few sections of this paper, this ternary blend is denoted as TB10. The processing of the blend was precisely defined.[32] In this way, the morphology of TB10 sample was controlled by the knowledge of both the competition between kinetics and phase separation thermodynamics in epoxy/thermoplastic mixture and the modifications of the interfacial tension between the phases that follow the addition of the compatibilizer. All details of the sample preparation were given in a previous paper.[33] TEM analysis[32,33] demonstrated that the introduction of MCDEA-*g*-K significantly reduces the interfacial tension, then leads to a decrease of particle size of the thermoplastic dispersed phase in the blend. Because of the absence, on micrographs, of a clear interface between the epoxy matrix and PPE, it was concluded that the addition of the emulsifier leads to the creation of an interphase. Obviously, the actual component of such an in situ synthesized interphase area cannot be separately synthesized.

3.2. Sample Characterization. Differential scanning calorimetry (DSC) thermograms were recorded using a DSC 7 Perkin-Elmer device with a heating rate of 10 °C/min under nitrogen atmosphere. The glass transition temperatures T_g's were determined from the slope change of the baseline.

The torsion pendulum micromechanalyzer [Metravib Company, Lyon, France] was used under isochronal conditions at three frequencies (0.01, 0.1, and 1 Hz) to measure the temperature dependence of the complex shear modulus G^* with a heating rate of ∼1 °C/min. The samples were approximately 34 mm long, 5 mm wide, and 0.8 mm thick.

4. Numerical Results and Discussion

4.1. Use of Mechanical Models in Direct Mode. Prediction of Mechanical Coupling Effects be-

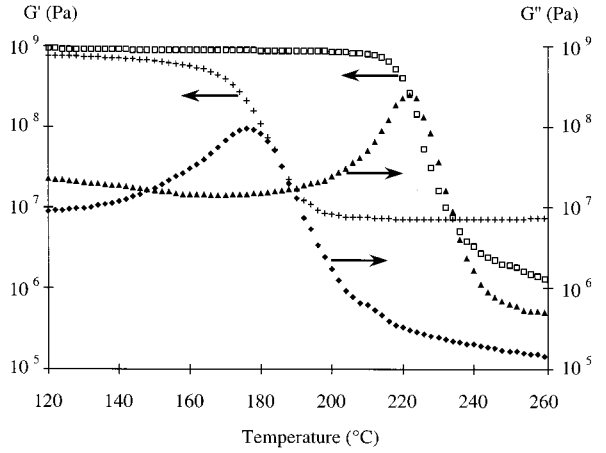

Figure 2. Viscoelastic characteristics (storage modulus G' and loss modulus G'') versus temperature at 1 Hz for DGEBA−MCDEA network (+, ◆) and PEI (□, ▲).

tween Phases. Mechanical properties of filled polymers are well-known to be governed by both the physicochemical interfacial interactions[5−8] and by the reinforcement effect,[8−15] the so-called mechanical coupling between phases. As a consequence, the sole mechanical coupling effects have first to be predicted before interpreting changes on the viscoelastic behavior of blended components. The magnitude of mechanical coupling effects in composite materials was earlier shown[8,12] to depend not only on mechanical properties and relative content of each phase but also on the geometric arrangement of the phases. In this way, this section focuses on the prediction of the magnitude of such reinforcement effects in the binary BB10 and BB20 thermoset/thermoplastic blends by accounting for the geometric arrangement of the different polymeric phases.

The mechanical behavior of such two-phase materials can be predicted by using Christensen and Lo's model[16] in direct mode. Numerical simulations are performed by accounting for the following assumptions:

- Viscoelastic properties of both thermoset and thermoplastic are taken to be identical to those displayed by pure DGEBA−MCDEA and PEI, respectively. The experimental real (G') and imaginary (G'') parts of the complex moduli for pure components are given in Figure 2.
- Volume fractions are chosen in agreement with blend composition, that is, 0.1 (or 0.2) for PEI and 0.9 (or 0.8) for DGEBA−MCDEA in BB10 (or BB20) sample.
- To account for the glassy−rubbery transition undergone by the polymers through their respective glass transition, an S-shape variation of the Poisson's ratio of both components is assumed from 0.33 to 0.50 at $T > T_g$.[8]

Accounting for the different morphologies, which are exhibited by BB10 and BB20 samples, two RVE-2 phases (Figure 1a) must be defined. They are denoted as RVE-1 and RVE-2, respectively. In RVE-1, the central core is constituted by a thermoplastic PEI inclusion with the radius R_{d1}, which is surrounded by a shell of thermoset DGEBA−MCDEA matrix that is limited by the spheres with the radii R_{d1} and R_{c1}. As given in eq 1, the ratios of radii are expressed as a function of the volume fractions of the dispersed phases (V_{p1}) and matrix (V_{m1}). In RVE-2, a thermoset inclusion, acting as the central core with the radius R_{d2} is embedded by a shell of thermoplastic matrix (limited

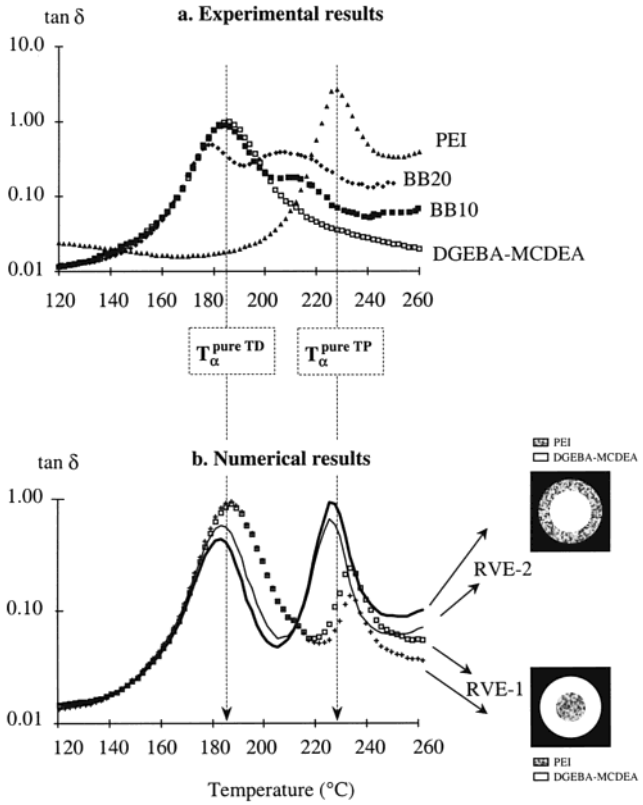

Figure 3. Evolution of the loss factor tan δ versus temperature at 1 Hz: (a) experimental viscoelastic behavior for DGEBA−MCDEA (□), PEI (▲), BB10 (■), and BB20 (◆). b. theoretical evolution for blends containing 90 (+, −) or 80 (□, —) vol % of DGEBA−MCDEA, which is considered in RVE as continuous phase (symbols, RVE-1) or dispersed phase (full lines, RVE-2). *The temperature locations T_α^{TD} and T_α^{TP} for pure components (given in Table 1) are indicated with arrows (from Figure 3a to Figure 3b) for comparison.*

by the spheres with the radii R_{d2} and R_{c2}). The ratios of radii also are expressed as a function of the volume fractions of the dispersed (V_{p2}) and continuous (V_{m2}) phases. It can be relevant to establish the relationship between the radii of concentric spheres, which are considered in RVE-1 and RVE-2. As a matter of fact, RVE-1 and RVE-2 can be used for a given blend composition, to better illustrate the influence of the geometric arrangement of phases on the mechanical coupling effects. This leads to $V_{p1} = V_{m2}$ and $V_{m1} = V_{p2}$. Accordingly, the radii R_{d1} and R_{c1} in RVE-1 can be connected to the radii R_{d2} and R_{c2} in RVE-2 by the following expression:

$$R_{d2} = R_{c2}\{1 - (R_{d1}/R_{c1})^3\}^{1/3} \qquad (6)$$

Figure 3a gives the experimental values of the loss factor (tan δ) at 1 Hz for all the materials, and Figure 3b reports theoretical evolution of tan δ at 1 Hz vs temperature for binary blends containing 10 or 20 vol % of PEI. Modeling was performed by considering either RVE-1 or RVE-2.

Now, it is of interest to compare theory and experiment. In this way, the following experimental characteristics are listed in Table 1:

- The T_g's (DSC measurements) of both thermoset and thermoplastic phases in BB10 and BB20 samples as well as T_g values of pure components (PEI and DGEBA−MCDEA network).

Table 1. Experimental Characteristics Concerning BB10 and BB20 Binary Blends, and Pure Components

	glass transition temp T_g (°C) from differential scanning calorimetry		characteristic issues from dynamic mechanical analysis at 1 Hz			
	thermoset phase	thermoplastic phase	thermoset phase		thermoplastic phase	
	T_g^{TD} (°C)	T_g^{TP} (°C)	T_α^{TD} (°C)	tan δ_{maxTD}	T_α^{TP} (°C)	tan δ_{maxTP}
DGEBA−MCDEA network	175 ± 2		186 ± 1	0.94		
BB10	166 ± 2	*a*	184 ± 1	0.70	208 ± 2	0.33
BB20	169 ± 2	180 ± 2	179 ± 1	0.39	210 ± 2	0.32
PEI		214 ± 2			228 ± 2	2.51

[a] Too weak a change in the heat capacity baseline to determine.

• The temperature location of the main relaxation (from Figure 3a) related to T_g for both thermoset and thermoplastic phases (denoted as T_α^{TD} and T_α^{TP}, respectively).

• The height of the corresponding peak (Figure 3a) of tan δ (denoted as tan δ_{max}), displayed by all the materials.

On one hand, it can be seen that T_g of thermoset phase in both BB10 and BB20 samples is located at about 168 °C, that is, at a lower temperature than T_g of the pure epoxy network. Such an observation probably results from a decrease in the cross-linking degree of the epoxy network in the blends. This could be induced by the phase separation of the thermoplastic during curing. It can be also seen that the T_g of thermoplastic phase is located at a lower temperature in BB20 sample than in pure PEI ($\Delta T \sim 30$ °C). This strong shift toward lower temperatures could be attributed to the remaining low molar masses epoxy−amine species dissolved in the thermoplastic phase, which act therefore as plasticizers.[31] This is consistent with a lower cross-linking degree of the epoxy network.

On the other hand, the analysis of experimental mechanical data leads to the following features:

• T_α^{TD} displayed by BB10 sample is very close to that of pure epoxy network. In contrast, a significant shift toward the lower temperatures is observed for T_α^{TD} in BB20 sample.

• T_α^{TP} values displayed by both BB10 and BB20 samples remain constant at about 209 °C, that is, at a lower temperature than that of pure PEI ($\Delta T \sim 20$ °C).

• Nevertheless, it is relevant to underline that the shifts toward the lower temperatures of both T_α^{TD} (mainly) and T_α^{TP} are significantly lower than T_g shifts found from DSC analysis.

Last, Figure 3b appears very interesting for investigating mechanical coupling effects between phases in polymer blends. It can be seen that

• The temperature location of the main relaxation related to T_g (denoted as T_α^{TD} and T_α^{TP} in Table 1) is governed by the accounted morphology in the modeling. As a matter of fact, by choosing the thermoset phase as the continuous phase (RVE-1), it can be observed a shift of both T_α^{TD} and T_α^{TP} toward higher temperatures compare to T_α values of pure DGEBA−MCDEA network and pure PEI, respectively. In contrast, when modeling is carried out by considering the thermoplastic phase as the continuous phase (RVE-2), a significant shift of both T_α^{TD} and T_α^{TP} of blends toward the lower temperatures compared to ones of pure components can be observed.

• For the same composition, the magnitude of the main relaxations exhibited by both thermoset and thermoplastic phases are the highest when the respective component is chosen as the continuous phase in modeling.

The magnitude of mechanical coupling effects between phases in polymer blends is therefore predicted to depend on the geometric arrangement of the phases.

Thus, the comparison of experimental and theoretical analysis leads to the following interpretations:

• For the BB10 sample, in which the thermoset component acts as the continuous phase, the theoretical approach predicts a shift of T_α^{TD} toward the higher temperatures. However, from experimental viscoelastic analysis, it was observed that T_α^{TD} in the BB10 sample is very close to T_α displayed by pure DGEBA−MCDEA network. Recalling also that DSC measurements revealed a shift of T_g toward the lower temperatures for the thermoset phase in the blend, it can be concluded that changes in microstructure and mechanical coupling effects act in opposite ways, leading to the weak change in the T_α^{TD} location in mechanical spectra.

• For the BB20 sample, the thermoplastic phase acts as the continuous phase. In this case, mechanical modeling predicts a shift of T_α^{TD} toward the lower temperatures. Thus, changes in microstructure (revealed by DSC measurements) and mechanical coupling act in similar ways, which leads to the significant shift toward lower temperatures observed in the T_α^{TD} location in mechanical spectra.

In this section, the viscoelastic properties of binary thermoset/thermoplastic polymer blends were investigated in connection with blend morphologies. By using Christensen and Lo's model in direct mode, it was shown that, as for composite materials, the magnitude of mechanical coupling effects between phases in polymer blends is predicted to depend not only on mechanical properties and relative content of each phase but also on the geometric arrangement of the phases accounted for in modeling. Thus, both experimental results and the accurate knowledge of mechanical coupling effects predicted by using direct mechanical modeling led to the unequivocal interpretation of a decrease in the cross-linking degree of the epoxy network in BB10 and BB20 samples.

Qualitative Probe of Blend Morphology. It is also relevant to demonstrate that both experimental viscoelastic data of heterogeneous polymeric materials (as well as those of pure components) and theoretical issues from mechanical modeling can be combined to probe the morphology of multiphase polymeric systems. In this way, numerous examples in the literature[34−37] reported that the knowledge of both evolution of absolute dynamic shear modulus G_d (defined as $G^*(T,f) = G_d(T,f)\, e^{i\delta(T,f)}$) and phase angle δ over a wide range of temperatures (T) and frequencies (f) can lead to the evaluation of morphological variation in a number of polymer blends. Thus, Eklind and Maurer[38] plotted δ vs G_d in order to explore the possibilities and limitations of determining the morphology of heterogeneous polymer

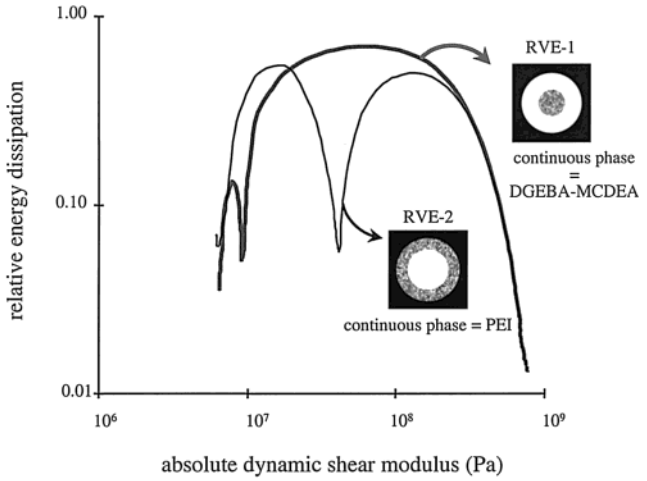

Figure 4. $\Delta W/W$ vs G_d plots from theoretical data given by using Christensen and Lo's model in direct mode with RVE-1 (—) or with RVE-2 (−).

blends by melt-state dynamic mechanical spectroscopy. They also compared experimental results with numerical simulations to discuss morphology of blends.

Such an approach also can be used for polymer blends at the solid state. As a matter of fact, a new way of presenting experimental dynamic mechanical data and simulations, by plotting the relative energy dissipation per cycle against the absolute dynamic shear modulus was introduced.[14] The relative energy dissipation was given by the ratio of the dissipated energy (ΔW) and the total energy (W) on one cycle of mechanical strain. Furthermore, ($\Delta W/W$) can be expressed as a function of the loss factor tan δ as follows:

$$\frac{\Delta W}{W} = 2\pi \frac{\tan \delta}{\sqrt{(1 + \tan^2 \delta)}} \qquad (7)$$

Obviously, such a new graph can be plotted by using either experimental viscoelastic data or theoretical issues from mechanical modeling. Therefore, as the morphology of multiphase materials is taken into account through the definition of the geometric arrangement of phases in the representative volume element (RVE), the comparison between both experimental and theoretical plots (issued from mechanical modeling based on several RVE) must be expected as an interesting probe of the morphology of samples. To demonstrate the ability of such an association of both theory and experiment, two illustrations are now given.

The first one concerns the above studied binary thermoset/thermoplastic blends. Accounting for the different morphologies exhibited by BB10 and BB20 samples, two representative volume elements (RVE-1 and RVE-2) were defined. For the same blend composition (here, 10 wt % of PEI, for example), Figure 4 reports the representations of the relative energy dissipation vs the absolute dynamic shear modulus from theoretical data obtained by considering either the DGEBA−MCDEA network (RVE-1) or PEI (RVE-2) as the continuous phase in the blends. It is of interest to notice that both evolutions, which only differ by the geometric arrangement considered in numerical simulations, are clearly shown to be different. In Figure 5, parts a and b, the experimental evolutions of ($\Delta W/W$) vs G_d for BB10 and BB20 samples are now compared to the ones theoretically determined by using Christensen and Lo's

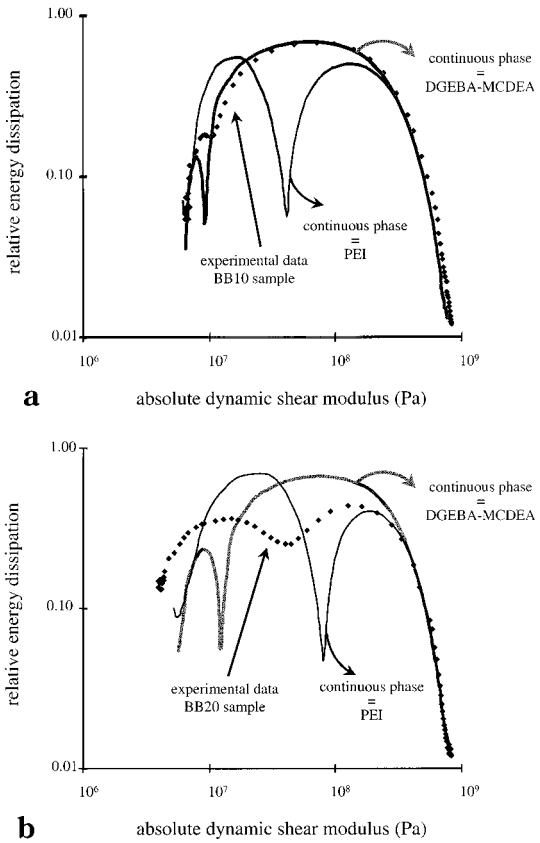

Figure 5. $\Delta W/W$ vs G_d plots from experimental (◆) and theoretical data given by mechanical modeling performed with RVE-1 (—) or with RVE-2 (−): (a) BB10 sample; (b) BB20 sample.

model in direct mode. For the BB10 sample (Figure 5a), a good agreement between experiment and theory when the thermoset is chosen as the continuous phase can be observed. In contrast, for the BB20 sample (Figure 5b), a good agreement is found between experimental evolution and theoretical data when considering PEI as the continuous phase. Such results agree with the previous investigation[31] of blend morphologies by transmission electron microscopy (TEM), and clearly shows the usefulness of such an approach for qualitatively describing the actual morphology of binary polymeric materials.

The second example concerns the three-phase in situ compatibilized thermoset/thermoplastic polymer blend, denoted as TB10. Because of the reactive aspect of the compatibilizer, the actual component of the in situ synthesized interphase area cannot be separately synthesized. Nevertheless, as the addition of the emulsifier MCDEA-*g*-K mainly leads to the decrease of particle size of the thermoplastic (PPE) dispersed phase, TB10 sample may be considered as a binary DGEBA−MCDEA (90 wt %)/PPE (10 wt %) blend. According to this first approximation, the mechanical behavior of such a two-phase material can be predicted by using Christensen and Lo's model. As for BB10 and BB20 samples, numerical simulations were performed by considering either RVE-1 or RVE-2. Obviously, the viscoelastic properties of PEI were replaced by those of PPE in the representative volume elements. Figure 6 shows both experimental and theoretical $\Delta W/W$ vs G_d plots for TB10 sample. Experimental plot is found to be close to theoretical one obtained by considering DGEBA−MCDEA as the continuous phase in modeling.

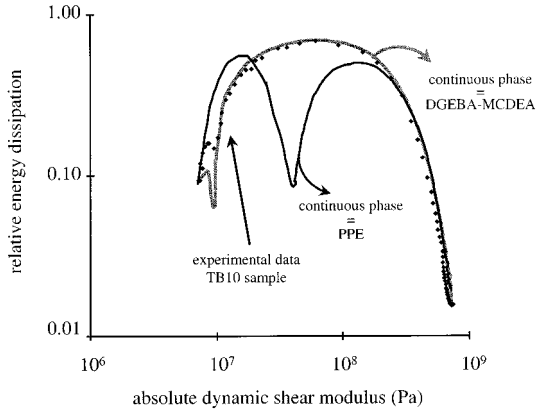

Figure 6. $\Delta W/W$ vs G_d plots from experimental and theoretical data concerning TB10 sample: (a) experimental data (◆); (b) Theoretical data obtained by using mechanical modeling with modified RVE-1 (—) and with RVE-2 (−), respectively.

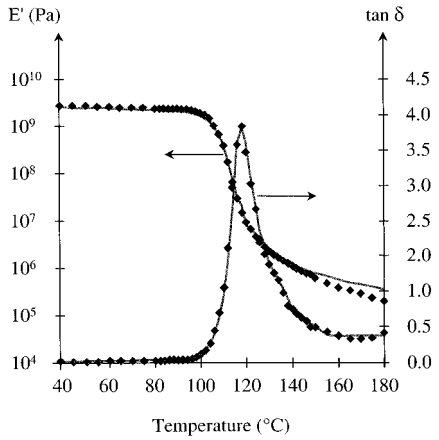

Figure 7. Viscoelastic characteristics (storage modulus E' and loss factor tan δ) vs temperature for the actual polystyrene matrix in PC15 sample as predicted by the reverse mechanical modeling (−) and for pure polystyrene experimentally recorded by mechanical spectrometry (◆).

This observation is in a great accordance with previous investigation of blend morphology by TEM.[32,33]

In this section, a new way of presenting experimental viscoelastic data and numerical simulations was detailed. Such a plot of the relative energy dissipation per cycle against the absolute dynamic shear modulus was demonstrated to be a sensitive qualitative probe of the morphology of the multiphase polymeric systems.

4.2. Use of Mechanical Models in Reverse Mode. The use of mechanical modeling in reverse mode was recently introduced.[13,25] By accounting for morphology, composition, and viscoelastic characteristics of pure components and those of blended system, such a new approach led successfully to the extraction of the actual viscoelastic properties of one phase among others in several multiphase polymeric materials.[13,25,26,28] The self-consistency of our approach was first demonstrated by investigating model systems[25,29] for which morphology, and viscoelastic properties as well as volume fractions of all components were exactly known. This section of the article focuses on the demonstration of the ability and the consistency of the reverse calculation whatever study of heterogeneous polymeric materials be. In this way, we propose to investigate the actual viscoelastic behavior of the following:

- the polystyrene matrix in PC15 sample;
- the in situ synthesized interphase in TB10 sample.

Extraction of the Actual Properties of PS Matrix in PC15 Sample. Morphology and viscoelastic properties of PC15 sample were previously investigated by Alberola and Mele.[12] The viscoelasticity of polystyrene reinforced by glass beads was accurately recorded by using a mechanical spectrometer [Metravib Company, Lyon, France]. Isochronal scans were performed at 5 Hz by increasing the temperature from 40 to 180 °C to measure the temperature dependence of the complex Young modulus E^*. Differential scanning calorimetry experiments showed that only 15 vol % of glass beads did not significantly affect the viscoelastic behavior of the polystyrene. Furthermore, scanning electron microscopy revealed that PS acts as the continuous phase in PC15 sample and that 15 vol % of glass beads do not lead to the percolation of the spherical particles.

As a consequence, Christensen and Lo's model can be used in reverse mode for investigating the mechanical behavior of PS matrix in such a two-phase composite material. Numerical simulations are performed by accounting for the following assumptions:

- Young's modulus and Poisson's ratio of glass beads are chosen to be constant over the analyzed temperature range and to be equal to 70GPa and 0.2, respectively.
- Volume fractions are chosen in agreement with the composition of the particulate composite, that is 0.15 for glass beads and 0.85 for PS.

It is also required to define a representative volume element of PC15 sample. This RVE-2 phases is constituted by two concentric spheres embedded in the equivalent homogeneous medium. In agreement with the morphology of PC15 sample, the central core is constituted by the glass beads and is surrounded by a shell of polystyrene matrix. The last input required to carry out the reverse calculation is the viscoelastic characteristics of PC15 sample.

In Figure 7, the actual viscoelastic behavior of the polystyrene matrix separated by using Christensen and Lo's model in reverse mode are associated with that of pure polystyrene which were separately experimentally recorded.[13] It can be shown that both experimental and reverse theoretical data almost are superimposed. Thus, in agreement with DSC measurements, such numerical results based on reverse mechanical modeling show that the viscoelastic behavior of PS matrix is not significantly influenced by 15 vol % of glass beads.

This first example mainly proves the accuracy of the reverse approach. The following one is now presented for giving evidence of the usefullness of the reverse way in the understanding of the overall properties of multiphase polymeric materials.

Extraction of the Actual Properties of the in Situ Synthesized Interphase in the TB10 Sample. The study of the interphases in multiphase polymeric materials remains an important subject of research, and it is well-known that the interphase properties strongly affect the actual properties of such materials. Although it seems obvious that the actual properties of the interfacial macromolecules differ from those of the pure components, their in situ detection and characterization remain a problem. Mechanical spectrometry and reverse mechanical modeling can be of interest for such a purpose. In this way, this section deals with the three-phase in situ compatibilized DGEBA−MCDEA/PPE polymer blend, whose actual component of the in situ synthesized interphase cannot be separately synthesized.

Morphology and viscoelastic properties of TB10 sample were previously investigated.[33] Mechanical spectrometry revealed an additional loss peak at about 60 °C at 1 Hz in the compatibilized blend spectrum which was detailed as a "micromechanical transition". According to Eklind and Maurer[39] such a transition, which did not correspond to a relaxation of one of the pure components, was predicted through direct mechanical modeling to depend on the Poisson's ratio and the volume fraction of the interphase. The occurrence of the "micromechanical transition" on mechanical spectra was also shown[33] to be significantly influenced by the thermal history of TB10 sample.

Since (1) the actual viscoelastic characteristics of the interphase are not experimentally accessible, and (2) the definition of the "micromechanical transition" mainly results from theoretical simulations, we propose to use the (3 + 1) phases self-consistent scheme in reverse mode to study the properties of the in situ synthesized interphase area. Such an investigation requires the definition of RVE-3 phases (Figure 1b) which is constituted by three concentric spheres embedded in the equivalent homogeneous medium. Thus, the central core (Phase 1) is constituted by the thermoplastic PPE inclusion, and surrounded by a shell of interphase (phase 2). Phase 2 is covered by a shell of thermoset DGEBA−MCDEA matrix. As given in eq 2, the radii of the shells are expressed as a function of the volume fractions of the phases. Reverse mechanical modeling was performed by considering as input data the viscoelastic characteristics for pure matrix, pure inclusion, and TB10 sample at 1 Hz. To perform the accurate separating of the characteristics of the interphase in a reasonable amount of computer time, we chose to consider the temperature range from 10 to 140 °C, i.e., the temperature range where the interphase relaxation was revealed.[33] In this temperature range, both thermoset matrix and thermoplastic inclusions are in the glassy state. That is why Poisson's ratios for vitreous matrix and inclusions were chosen to be equal to 0.33 and that of the interphase component was chosen to be equal to 0.50. In so far as simulations[39] predicted that the location of a "micromechanical transition" depends on the Poisson's ratio of the interphase, we also tested various values for the Poisson's ratio of the interphase ranging from 0.33 to 0.50. No significant change was detected in the predicted data which were derived from the reverse mechanical modeling. The last input which is required for the reverse mechanical modeling is the composition of the blend. All numerical results here given were performed for a volume fraction equal to 0.10 for the thermoplastic inclusions. The effective volume fraction of the interphase component being unknown, the reverse mechanical modeling were performed for volume fractions of interphase equal to 0.015, 0.020, 0.030, 0.050, and 0.070. The volume fraction of the thermoset matrix was then chosen by considering the sum of the volume fractions to be equal to 1.

Theoretical issues from the reverse mechanical modeling performed at 1 Hz are given in Figure 8, parts a and b, which shows the evolution of both predicted storage modulus and predicted loss factor tan δ vs temperature for the various contents of interphase. It can be seen in Figure 8a that the storage modulus depends on the value chosen for the volume fraction of the interphase. The higher the volume fraction of the interphase is, the higher are the predicted values of the

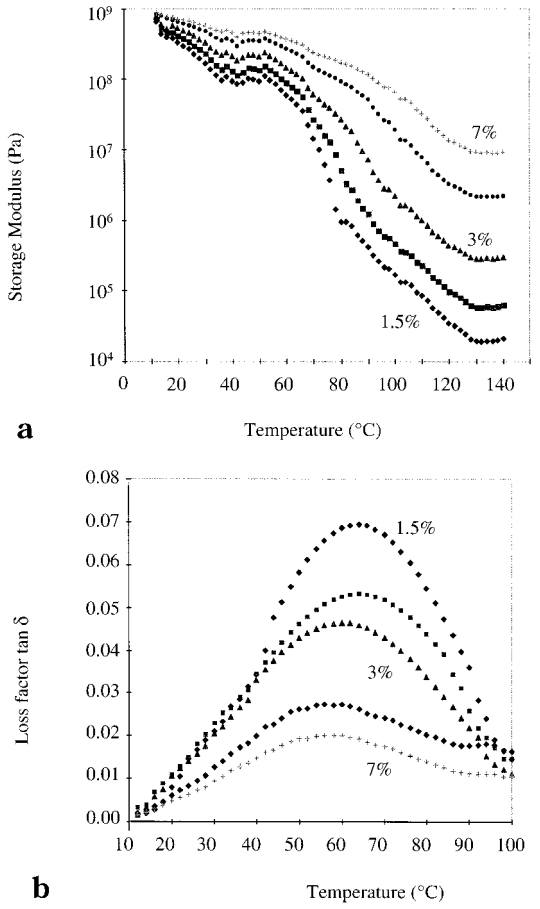

Figure 8. Theoretical viscoelastic characteristics at 1 Hz for the in situ synthesized interphase as a function of the effectively considered amount of interphase in TB10 sample: (◆) 1.5% interphase in the blend, (■) 2%, (▲) 3%, (◆) 5%, or (+) 7%.

storage modulus. This result mainly reflects the properties of the reverse mechanical approach: these lead logically to the greatest evolution of interfacial properties for the lowest amount of interphase component. Nevertheless, whatever the volume fraction of the interphase can be, predicted storage modulus curves follow the same tendency. First, a significant decrease of these values is shown from 10 to about 130 °C. Then, the predicted storage modulus appears constant on average. Such a viscoelastic behavior corresponds to that of a rubbery material, which is consistent with chemical composition of the interphase component mainly containing poly(ethylene-*co*-butene). Figure 8b reveals that the predicted loss factor tan δ shows a maximum and depends on the assumed volume fraction of the interphase. Thus, it can be seen that the magnitude of the peak significantly decreases when the effectively considered volume fraction of interphase increases. Subsequently, the temperature location of the maximum is slightly decreased from 65 to 58 °C for volume fraction ranging from 0.01 to 0.07.

Such theoretical data based on reverse mechanical modeling confirm the interpretation of the additional peak in experimental mechanical spectrum at about 60 °C as a "micromechanical transition". As a matter of fact, such a transition is well-known[22,29,39] as resulting from the combined influence of the microstructure of the multiphase polymeric material including an interphase and the relative temperature-dependent moduli of the

blended components which is induced by the important molecular mobility in the interphase area.

In this section, both accuracy and usefulness of reverse mechanical modeling were evidenced. Such a new approach for mechanical modeling was shown to be of particular interest for the study of the actual properties in the interfacial area of multiphase polymeric materials.

5. Conclusion

Mechanical modeling and dynamic mechanical analysis were detailed as tools for extracting information about morphology, molecular mobility, and interfacial interactions in multiphase polymeric materials. Such an investigation required the use of self-consistent mechanical models in direct and reverse modes. The ability of both direct and reverse approaches was demonstrated through the study of several heterogeneous polymeric systems, whose viscoelastic properties were investigated in connection with their morphologies.

Thus, mechanical coupling effects in binary thermoset/thermoplastic polymer blends were highlighted by using Christensen and Lo's model in direct mode. First, the magnitude of these effects between phases in such blends, as in composite materials, was shown to depend not only on mechanical properties and relative content of each phase but also on the geometric arrangement of the polymeric phases. Then, it was demonstrated that, in some cases, microstructural modifications in blended materials can be screened by mechanical coupling effects. This result underlines the fact that it is first necessary to investigate the sole effects resulting from mechanical coupling between phases before interpreting experimental mechanical spectra of multiphase polymeric systems.

Subsequently, a new way of presenting experimental dynamic mechanical data and simulations by plotting the relative energy dissipation per cycle against the absolute dynamic shear modulus was shown to be a qualitative probe of the morphology of multicomponent materials.

Last, the extraction of the actual viscoelastic properties of one phase among others in several multiphase polymeric systems was investigated by using reverse mechanical modeling. Such a new way was shown to be of particular interest for investigating the actual viscoelastic properties of interphases in compatibilized multiphase materials.

Appendix

1. The solution for the complex shear modulus, $G^*_{2\ \text{phases}}$, of the two-layered concentric sphere is given by the resolution of the following quadratic equation:

$$A_{2\ \text{phases}}\left[\frac{G^*_{2\ \text{phases}}}{G^*_c}\right]^2 + B_{2\ \text{phases}}\left[\frac{G^*_{2\ \text{phases}}}{G^*_c}\right] + C_{2\ \text{phases}} = 0$$

where

$$A_{2\ \text{phases}} = 8\left(\frac{G_d}{G_c} - 1\right)(4 - 5\nu_c)\eta_1 V_d^{10/3} - 2\left[63\left(\frac{G_d}{G_c} - 1\right)\eta_2 + 2\eta_1\eta_3\right]V_d^{7/3} + 252\left(\frac{G_d}{G_c} - 1\right)\eta_2 V_d^{5/3} - 50\left(\frac{G_d}{G_c} - 1\right)(7 - 12\nu_c + 8\nu_c^2)\eta_2 V_d + 4(7 - 10\nu_c)\eta_2\eta_3$$

$$B_{2\ \text{phases}} = -4\left(\frac{G_d}{G_c} - 1\right)(1 - 5\nu_c)\eta_1 V_d^{10/3} - 4\left[63\left(\frac{G_d}{G_c} - 1\right)\eta_2 + 2\eta_1\eta_3\right]V_d^{7/3} - 504\left(\frac{G_d}{G_c} - 1\right)\eta_2 V_d^{5/3} + 150\left(\frac{G_d}{G_c} - 1\right)(3 - \nu_c)\eta_2\nu_c V_d + 3(15\nu_c - 7)\eta_2\eta_3$$

$$C_{2\ \text{phases}} = 4\left(\frac{G_d}{G_c} - 1\right)(5\nu_c - 7)\eta_1 V_d^{10/3} - 2\left[63\left(\frac{G_d}{G_c} - 1\right)\eta_2 + 2\eta_1\eta_3\right]V_d^{7/3} - 252\left(\frac{G_d}{G_c} - 1\right)\eta_2 V_d^{5/3} + 25\left(\frac{G_d}{G_c} - 1\right)(\nu_c^2 - 7)\eta_2 V_d - (7 + 5\nu_c)\eta_2\eta_3$$

with ν_c and ν_d are the Poisson ratios of the continuous and the dispersed phases, respectively

$$\eta_1 = (49 - 50\nu_c\nu_d)\left(\frac{G_d}{G_c} - 1\right) + 35\frac{G_d}{G_c}(\nu_d - 2\nu_c) + 35(2\nu_d - \nu_c)$$

$$\eta_2 = 5\nu_d\left(\frac{G_d}{G_c} - 8\right) + 7\left(\frac{G_d}{G_c} + 4\right)$$

$$\eta_3 = \frac{G_d}{G_c}(8 - 10\nu_c) + (7 - 5\nu_c)$$

2. The solution for the complex shear modulus, $G^*_{3\ \text{phases}}$, of the three-layered concentric sphere is given by the resolution of the following quadratic equation:

$$A_{3\ \text{phases}}\left[\frac{G^*_{3\ \text{phases}}}{G^*_3}\right]^2 + B_{3\ \text{phases}}\left[\frac{G^*_{3\ \text{phases}}}{G^*_3}\right] + C_{3\ \text{phases}} = 0$$

where

$$A_{3\ \text{phases}} = 4R_3{}^{10}(1-2\nu_3)(7-10\nu_3)Z_{12} + 20R_3{}^7(7-12\nu_3+8\nu_3{}^2)Z_{42} + 12R_3{}^5(1-2\nu_3)(Z_{14}-7Z_{23}) + 20R_3{}^3(1-2\nu_3)^2Z_{13} + 16(4-5\nu_3)(1-2\nu_3)Z_{43}$$

$$B_{3\ \text{phases}} = 3R_3{}^{10}(1-2\nu_3)(15\nu_3-7)Z_{12} + 60R_3{}^7(\nu_3-3)\nu_3Z_{42} - 24R_3{}^5(1-2\nu_3)(Z_{14}-7Z_{23}) - 40R_3{}^3(1-2\nu_3)^2Z_{13} - 8(1-5\nu_3)(1-2\nu_3)Z_{43}$$

$$C_{3\ \text{phases}} = -R_3{}^{10}(1-2\nu_3)(15\nu_3-7)Z_{12} + 10R_3{}^7(7-\nu_3{}^2)Z_{42} + 12R_3{}^5(1-2\nu_3)(Z_{14}-7Z_{23}) + 20R_3{}^3(1-2\nu_3)^2Z_{13} - 8(7-5\nu_3)(1-2\nu_3)Z_{43}$$

with

$$Z_{\alpha\beta} = P_{\alpha1}{}^{(n-1)}P_{\beta2}{}^{(n-1)} - P_{\beta1}{}^{(n-1)}P_{\alpha2}{}^{(n-1)} \quad \text{where} \quad \alpha \in [1,4],\ \beta \in [1,4] \quad \text{and} \quad n=3,\ k=2\ P^{(n)} = \prod_{j=1}^{n} M^{(j)}$$

and

$$M^{(k)} = \frac{1}{5(1-\nu_{k+1})} \times \begin{bmatrix} \frac{c^*_k}{3} & R_k{}^2\frac{(3b^*_k - 7c^*_k)}{5(1-2\nu_k)} & -12\frac{\alpha^*_k}{R_k{}^5} & \frac{4(f^*_k - 27^*\alpha_k)}{15R_k{}^3(1-2\nu_k)} \\ 0 & \frac{(1-2\nu_{k+1})b^*_k}{7(1-2\nu_k)} & -\frac{20(1-2\nu_{k+1})\alpha^*_k}{7R_k{}^7} & \frac{-12(1-2\nu_k)\alpha^*_k}{7R_k{}^5(1-2\nu_k)} \\ \frac{R_k{}^5\alpha^*_k}{2} & -R_k{}^7\frac{(2a^*_k + 147\alpha^*_k)}{70(1-2\nu_k)} & \frac{d^*_k}{7} & \frac{R_k{}^2(105(1-\nu_{k+1}) + 12\alpha^*_k(7-10\nu_{k+1}) - 7e^*_k)}{35(1-2\nu_k)} \\ -\frac{5}{6}(1-2\nu_{k+1})R_k{}^3\alpha^*_k & \frac{7(1-2\nu_{k+1})R_k{}^5\alpha^*_k}{2(1-2\nu_k)} & 0 & \frac{(1-2\nu_{k+1})e^*_k}{3(1-2\nu_k)} \end{bmatrix}$$

$$a^*_k = \frac{G^*_k}{G^*_{k+1}}(7+5\nu_k)(7-10\nu_{k+1}) - (7-10\nu_k)(7+5\nu_{k+1})$$

$$b^*_k = 4(7-10\nu_k) + \frac{G^*_k}{G^*_{k+1}}(7+5\nu_k)$$

$$c^*_k = (7-5\nu_{k+1}) + 2\frac{G^*_k}{G^*_{k+1}}(4-5\nu_{k+1})$$

$$d^*_k = (7+5\nu_{k+1}) + 4\frac{G^*_k}{G^*_{k+1}}(7-10\nu_{k+1})$$

$$e^*_k = 2(4-5\nu_k) + \frac{G^*_k}{G^*_{k+1}}(7-5\nu_k)$$

$$f^*_k = (4-5\nu_k)(7-5\nu_{k+1}) - \frac{G^*_k}{G^*_{k+1}}(4-5\nu_{k+1})(7-5\nu_k)$$

$$\alpha^*_k = \frac{G^*_k}{G^*_{k+1}} - 1$$

References and Notes

(1) Yu, A. J. In *Multicomponent Polymer Systems*; N. A. J. Platzer: Washington, DC, 1971.

(2) Gaylord, N. G. In *Copolymers, Polyblends and Composites*; N. A. J. Platzer: Washington, DC, 1975.

(3) Gedde, U. W. In *Polymer Physics*; Chapman & Hall: London, 1995.

(4) Lipatov, Y. S. In *Physical Chemistry of Filled Polymers*; Monograph No. 2; Institute of Polymer Science and Technology, British Library: London, 1979.

(5) Dickie, R. A. In *Polymer Blends*; Paul, D. R., Newman, S.; Eds.; 1978; Vol. 1; Chapter 8.

(6) Shalaby, S. W. In *Thermal Characterization of polymeric materials*; Turi, E. A.; Ed.; Academic Press: London, 1981.
(7) Thomason, J. L. In *Interfaces in Polymer, Ceramic and Metal Matrix Composites*; Ishida, H.; Ed.; Elsevier Science: New York, 1988.
(8) Alberola, N. D.; Fernagut, F.; Mele, P. *J. Appl. Polym. Sci.* **1997**, *63*, 1029.
(9) Reed, K. E. *Polym. Compos.* **1980**, *1*, 44.
(10) Theocaris, P. S. *Adv. Polym. Sci.* **1985**, *66*, 149.
(11) Lipatov, Y. S. *Adv. Polym. Sci.* **1977**, *22*, 1.
(12) Alberola, N. D.; Mele, P. *Polym. Compos.* **1996**, *17*, 751.
(13) Alberola, N. D.; Merle, G.; Benzarti, K. *Polymer* **1999**, *40*, 315.
(14) Colombini, D.; Merle, G.; Alberola, N. D. *J. Appl. Polym. Sci.* **2000**, *76*, 530.
(15) Bohn, L. *Adv. Chem. Ser.* **1974**, *142*, 66.
(16) Christensen, R. M.; Lo, K. H. *J. Mech. Phys. Solids* **1979**, *27*, 315.
(17) Herve, E.; Zaoui, A. *Int. J. Eng. Sci.* **1993**, *31*, 1.
(18) Takayanagi, M.; Okamoto, T. *J. Polym. Sci.* **1968**, *23*, 597.
(19) Voigt, V. *Lehrbuch der Kristall Physik*; Teuber, B. G.: Berlin, 1910.
(20) Reuss, A. *Z. Angew. Math. Mech.* **1929**, *49*, 9.
(21) Hashin, Z.; Shtrickman, S. *J. Mech. Phys. Solids* **1963**, *11*, 127.
(22) Eklind, H.; Maurer, F. H. J. *J. Appl. Polym. Sci., Phys. Ed.* **1996**, *34*, 1569.
(23) Ouali, N.; Cavaille, J. Y.; Perez, J. *J. Plast. Rubber Compos. Process. Appl.* **1991**, *16*, 55.
(24) Maurer, F. H. J. In *Controlled Interphases in Composite Materials*; Ishida, H., Ed.; Elsevier Science: New York, 1990.
(25) Colombini, D.; Merle, G.; Alberola, N. D. *J. Macromol. Sci.—Physics* **1999**, *B38*, 957.
(26) Vendramini, J.; Mele, P.; Merle, G.; Alberola, N. D. *J. Appl. Polym. Sci.* **2000**, *77*, 2513.
(27) Dickie, R. A. *J. Polym. Sci.* **1976**, *17*, 45.
(28) Colombini, D.; Merle, G.; Alberola, N. D. *Macromol. Symp.* **2001**, *169*, 235.
(29) Colombini, D. Ph.D. Thesis, INSA, Lyon, France, 1999; http://csidoc.insa-lyon.fr/these/1999/colombini.
(30) Girard-Reydet, E.; Riccardi, C.; Sautereau, H.; Pascault, J. P. *Macromolecules* **1995**, *28*, 7608.
(31) Girard-Reydet, E.; Vicard, V.; Pascault, J. P.; Sautereau, H. *J. Appl. Polym. Sci.* **1997**, *65*, 2433.
(32) Girard-Reydet, E.; Sautereau, H.; Pascault, J. P. *Polymer* **1999**, *40*, 1677.
(33) Colombini, D.; Martinez-Vega, J. J.; Merle, G.; Girard-Reydet, E.; Pascault, J. P.; Gerard, J. F. *Polymer* **1999**, *40*, 935.
(34) Utracki, L. A.; Sammut, P. *Polym. Eng. Sci.* **1988**, *28*, 1405.
(35) Kim, B. K.; Jeong, H. M.; Lee, Y. H. *J. Appl. Polym. Sci.* **1990**, *40*, 1805.
(36) Kole, S.; Bhattacharya, A.; Tripathy, D. K.; Bhowmick, A. K. *J. Appl. Polym. Sci.* **1993**, *48*, 529.
(37) Baek, D. H.; Han, C. D. *Macromolecules* **1992**, *25*, 3706.
(38) Eklind, H.; Maurer, F. H. J. *Polym. Networks Blends* **1995**, *5* (1), 35.
(39) Eklind, H.; Maurer, F. H. J. *Polymer* **1996**, *37*, 2641.

MA010076V